INVESTIGATIONS ON PHYSICAL AND BIOLOGICAL RANGE UNCERTAINTIES IN KRAKÓW PROTON BEAM THERAPY CENTRE[*]

A. Rucinski[a], J. Baran[a], G. Battistoni[b,c], A. Chrostowska[d]
M. Durante[e,f], J. Gajewski[a], M. Garbacz[a], K. Kisielewicz[d]
N. Krah[g], V. Patera[h], M. Pawlik-Niedźwiecka[a,i], I. Rinaldi[j]
B. Rozwadowska-Bogusz[d], E. Scifoni[c], A. Skrzypek[a]
F. Tommasino[c,k], A. Schiavi[h], P. Moskal[i]

[a]Institute of Nuclear Physics Polish Academy of Sciences, Kraków, Poland
[b]INFN, Milan, Italy
[c]TIFPA, Trento, Italy
[d]Oncology Center Maria Skłodowska-Curie Memorial Institute
Kraków Branch, Poland
[e]Biophysics Department, GSI Helmholtzzentrum für Schwerionenforschung
Darmstadt, Germany
[f]Technische Universität Darmstadt, Institut für Festkörperphysik
Darmstadt, Germany
[g]University Lyon, CNRS, CREATIS UMR 5220, Centre Leon Berard
Lyon, France
[h]Sapienza University of Rome, Rome, Italy
[i]M. Smoluchowski Institute of Physics, Jagiellonian University, Kraków, Poland
[j]ZonPCT/Maastro clinic, Maastricht, The Netherlands
[k]University of Trento, Trento, Italy

Physical and biological range uncertainties limit the clinical potential of Proton Beam Therapy (PBT). In these proceedings, we report on two research projects, which we are conducting in parallel and which both tackle the problem of range uncertainties. One aims at developing software tools and the other at developing detector instrumentation. Regarding the first, we report on our development and pre-clinical application of a GPU-accelerated Monte Carlo (MC) simulation toolkit Fred. Concerning the letter, we report on our investigations of plastic-scintillator-based PET detectors for particle therapy delivery monitoring. We study the feasibility of Jagiellonian-PET detector technology for proton beam therapy range monitoring by means of MC simulations of the β^+ activity induced in a phantom-by-proton beams and present preliminary results of PET image reconstruction. Using a GPU-accelerated Monte Carlo simulation toolkit Fred and plastic-scintillator-based PET detectors, we aim at improving the patient treatment quality with protons.

---

1. Introduction

The increasing numbers of proton facilities and successful proton treatments [1] indicate that the relevance of Proton Beam Therapy (PBT) as a technique for tumor radiation therapy is rapidly growing. Kraków proton facility has been in clinical operation since October 2016 and more than 10 patients a day are currently treated.

Range uncertainties, *i.e.* uncertainty of the distance that protons travel inside patient body, currently represent one of the biggest caveats for the exploitation of the full potential of proton therapy treatments [2]. The proton-beams range is particularly affected by biological and physical uncertainties in a heterogeneous patient body. Therefore, to assure target coverage, medical physicists currently apply up to about 1 cm safety margins around the tumor volume, which lead to the unwanted irradiation of the healthy tissues surrounding the tumor [2].

The biological dose, D_{RBE} expressed in Gy(RBE), delivered to the patient is the actual quality of clinical interest. It is calculated as $D_{\mathrm{RBE}} = D \times \mathrm{RBE}$, where D is the physical dose expressed in Gy and RBE is the Relative Biological Effectiveness. By definition, in conventional therapy with photons RBE = 1.0, therefore, physical and biological doses are equal and correlated with clinical response. Protons have an increased biological effectiveness compared to photons, *i.e.* RBE is larger than one. Currently, in clinical routine, the RBE of protons is assumed to be constant and equal to 1.1 [3]. This convention neglects complex, often nonlinear dependency of the RBE on such parameters as penetration depth, Linear Energy Transfer (LET), dose, fractionation scheme, tissue type and endpoint, cell cycle phase or oxygenation level. These dependencies might affect the effective proton range, *i.e.*, introduce biological range uncertainty and thus affect the dose to the surrounding tissue and Organs at Risk (OAR). Modification of proton physical dose by RBE, which is an uncertain weighting factor, makes the correlation of proton biological dose and clinical effect of tumor irradiation uncertain, and unification of clinical studies comparing the effectiveness of different radiation modalities challenging.

An improvement resulting from the correctly applying radiobiological assumptions in PBT could be achieved only under the condition that the physical dose is accurately delivered to the patient. In fact, physical range uncertainties, occurring due to patient mispositioning or Computed Tomography (CT) scanner calibration introducing Hounsfield Unit (HU) to stopping power conversion, could cause differences between treatment plan and treatment delivery. Monte Carlo simulations and range monitoring methods are essential in PBT to guarantee that the physical dose is accurately delivered and, therefore, to reduce the biological and physical range uncertainties in a patient body.

Figure 1 illustrates which role could play each of the two topics reported in this manuscript in the clinical treatment workflow.
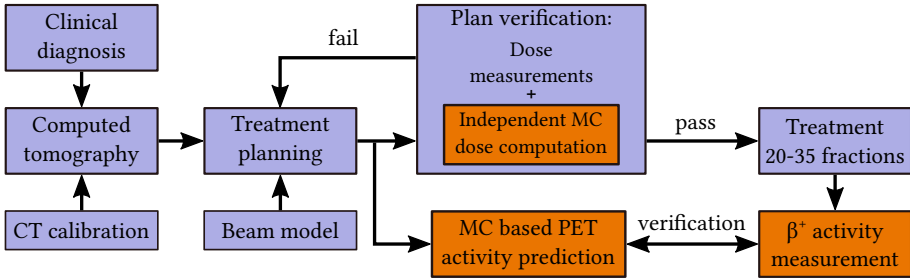

Fig. 1. Diagram of the standard patient treatment protocol (light gray/blue colors) along with activities of our group (dark gray/orange color) aiming to improve PBT quality. We incorporate advanced nuclear physics computational and experimental methods to predict physical and biological dose in patient more accurately and to monitor proton beam range in patient by means of PET imaging.

2. Monte Carlo simulations to address physical and biological range uncertainties of proton beams

It is recognized that Monte Carlo (MC) methods can offer improved dose calculation accuracy in heterogeneous media and, therefore, predict more accurately therapeutic dose distributions in patients compared to the analytical algorithms that are typically employed in the Treatment Planning Systems (TPS) used in clinical routine [2]. Nowadays, the use of a variable RBE is being discussed among the PBT scientific community. We perform biological dose calculations with variable RBE and investigate biological range uncertainties by means of MC simulations of patient CT images exploiting the MC dose calculation tool Fred [4, 5]. Fred offers a unique combination of features: accuracy of an MC code including biological dose computation, flexibility of a research tool, and high-dose calculation speed due to GPU-acceleration. These characteristics are impossible to achieve with the currently available commercial TPS and general purpose MC codes such as Geant4/FLUKA [6, 7].

We have successfully implemented in Fred the proton beam model used clinically for patient treatment in the Kraków facility. The Integrated Depth Dose (IDD) profiles of single proton pencil beams in water simulated with Fred MC code for different energies are in excellent agreement with the IDDs obtained during the commissioning measurements (see Fig. 2, left), showing differences of less than 2%.
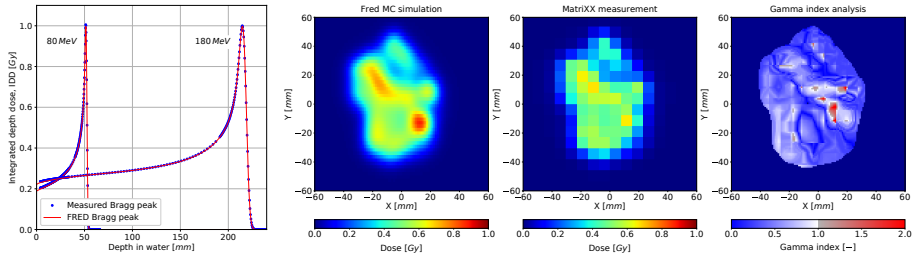
Fig. 2. Integrated depth dose distributions of proton pencil beams simulated in Fred and obtained experimentally during the facility commissioning (left), an example of transversal 2D dose distribution in isocentre plane obtained from Fred MC simulations (middle left), measured with MatriXX detector in water (middle right) and a GI map computed from simulation and measurement using GI (3%/2 mm) method (right). GI passing rate is 98.64%.

The emittance model, describing lateral beam propagation in air, was implemented in Fred, in accordance with the clinical system. The longitudinal and lateral pencil beam shapes are modeled in Fred MC with a submillimeter precision.

We validated the beam model experimentally using the transversal patient treatment plan verification measurements. Such measurements are routinely performed by medical physicists for treatment plan quality assurance with an array of 1020 ionization chambers (MatriXX IBA) placed in a water phantom. A transversal dose plane extracted from Fred MC and the dose distribution measured with the MatriXX detector at the same depth in water, as well as the Gamma Index (GI) map obtained from GI test are presented in Fig. 2. The GI passing rate (3%/2 mm criteria) greater than 98% was obtained for 182 dose planes measurements for 10 patients. Based on these results, we can assure that dose distributions of clinical treatment plans can be recalculated accurately.

We are currently performing treatment planning studies to quantify the biological range uncertainties exploring various biological models with variable RBE and clinical data of patients treated in Kraków.

An example of a selected Head and Neck (H&N) patient is presented in Fig. 3, where the radiobiological dose distributions computed with constant and variable RBE using Fred as well as corresponding Dose Volume Histograms (DVHs) are shown. The MC calculation time for this case was about 10 min (9×10^8 primary protons, $2 \times 10^6 \frac{p^+}{s}$ tracking rate). The mean dose to Planning Target Volume (PTV), calculated with Fred using variable RBE model proposed by Carabe [8], is increased with respect to the clinically applied constant RBE = 1.1 assumption of about 3 Gy(RBE), whereas the maximum dose to the brain stem OAR increases by about 4 Gy(RBE). Our results show that incorporation of the variable RBE model in patient

dose calculation increases the dose in PTV and OAR with respect to constant RBE assumption. This is especially important when OARs are very close to or overlap with the PTV as it occurs frequently in H&N patients. Considering variable RBE hypothesis in the proton therapy clinic could be essential as the increased biological dose deposited to OARs that exceeds clinical dose constraints can be potentially associated with the increased normal tissue complication probability and, therefore, an increased risk of necrosis or secondary cancer.
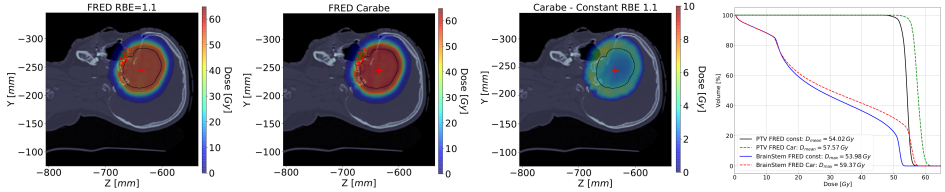
Fig. 3. Left: the RBE-weighted dose with constant RBE = 1.1, middle-left: the RBE-weighted dose with variable RBE (Carabe model [8]), middle-right: dose difference between constant and variable RBE. DVH for constant and variable RBE for PTV and brain stem.

The use of the fast MC dose computation tool Fred for physical and biological dose recalculation of patient treatment plans (retrospectively and prospectively) can provide additional clinical information for medical physicists and medical doctors, and can potentially prevent inaccuracies in patient treatment.

3. J-PET detector to address physical range uncertainties of proton beams

The proton interactions with patient tissues allow range monitoring during or just after the treatment detecting emitted secondary radiation. Tracking of prompt-gamma, PET-gamma, and secondary protons and neutrons are examples [9–11]. Prototype systems for prompt-gamma and PET-gamma range monitoring were tested clinically and obtained satisfying precision of Bragg peak position monitoring on-line in the PBT treatment room [12–14]. At the Jagiellonian University in Kraków, a novel solution for diagnostic PET imaging, Jagiellonian-PET (J-PET) is being developed [15–18].

A single detection unit of the J-PET scanner [19] consists of a 50 cm long and 6×24 mm^2 intersection size scintillator strip. The light pulses produced in the strip by 511 keV back-to-back photons propagate to its edges, where they are converted into electrical signals by photomultipliers (PMT). The interaction position of the photon with the detector is estimated from the time difference between the PMT signals located at the ends of the strip.

A J-PET module consists of 13 scintillator strips read-out through a single front-end electronics and an FPGA-based DAQ system. A modular, lightweight and portable design of J-PET enables flexibility in detector configuration and easy installation. Increasing the number of J-PET detector layers, increases the detection efficiency of the system.

We performed comprehensive MC simulations using the GATE toolkit [20] and reconstructions of 3D β^+ activity distributions using the CASTOR software [21]. The aim was to characterize the sensitivity of the J-PET for proton beam range detection. We investigated single and multi-layer cylindrical and dual-head configurations of the J-PET modules that can be possibly applied for the in-room range monitoring. The list-mode TOF-MLEM reconstruction (5 iterations with 500 ps TOF resolution without regularization) takes into account random events, scatter, attenuation and normalization corrections. Eventually, the reconstructed PET-activity profiles can be correlated with the position of dose distal fall-off (Fig. 4, right) and used for proton beam range monitoring.
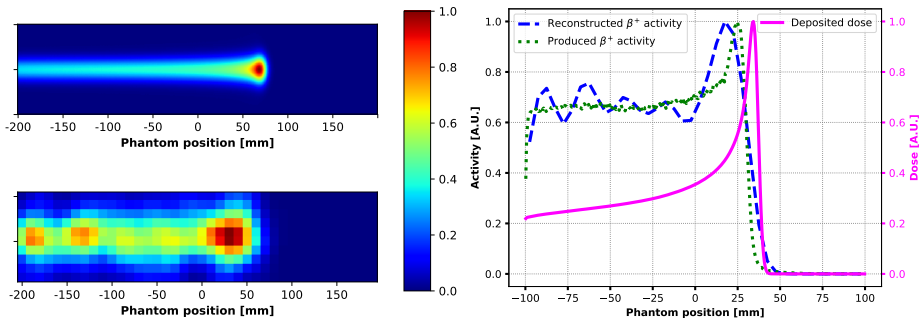

Fig. 4. The results of MC simulations. Top left: 2D distribution of dose deposited by 150 MeV proton beam in PMMA phantom; bottom left: β^+ activity distribution detected in J-PET and reconstructed with CASTOR software; right: dose, β^+ production in PMMA, reconstructed signal from β^+ activity detected with J-PET.

In this manuscript, we present preliminary results for one of the investigated setup configurations, *i.e.* a single layer J-PET barrel (Fig. 5). Figure 4 illustrates a cross section through the centre of the beam of 3D dose distribution deposited in a $5 \times 5 \times 20 \, \text{cm}^3$ PMMA phantom by 10^8 protons of nominal energy 150 MeV (top left) and the same cross section of reconstructed 3D distribution of β^+ activity produced by the beam in the phantom (bottom left). The activity map was reconstructed in the $5 \times 5 \times 5 \, \text{mm}^3$ voxel grid. The scintillator strips' detection efficiency is taken into account in MC simulations. The expected spatial and time resolutions of J-PET with wavelength-shifting strips (WLS) [22] is taken into account through plastic length discretization used in the simulations and image reconstruction.
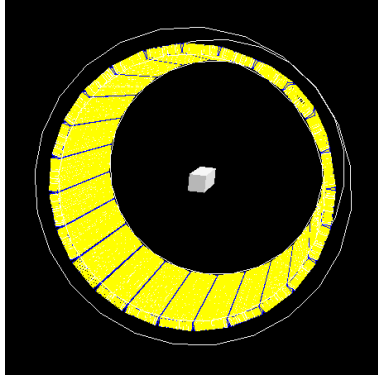
Fig. 5. Single-layer modular J-PET barrel with isocentrically positioned PMMA phantom.

Figure 4 (right) presents the MC simulated profiles of: *(i)* proton dose deposition in the PMMA phantom, *(ii)* β^+ activity produced in the phantom, and *(iii)* actual signal detected by J-PET barrel from β^+ activity. The results show that the J-PET detector is feasible to acquire the β^+ activity produced during proton therapy treatment and that the offline 3D reconstruction of PET activity images is possible using the CASTOR toolkit. The characterization of J-PET sensitivity for proton beam range detection is currently an ongoing research activity.

4. Summary

Within the research projects conducted in the Institute of Nuclear Physics Polish Academy of Sciences in Kraków, we investigate physical and biological range uncertainties of proton beams through positron emission tomography (PET) based solutions and Monte Carlo (MC) simulations. Taking advantage of the Fred accuracy and time performance possible due to the GPU acceleration, we aim at improving quality assurance and treatment planing in Kraków PBT facility. A Monte Carlo study of J-PET detector feasibility performed in the frame of the project suggests that this technique might be considered as a novel proton beam therapy range monitoring approach.

REFERENCES

[1] M. Durante, R. Orecchia, J.S. Loeffler, *Nat. Rev. Clin. Oncol.* **14**, 483 (2017).

[2] H. Paganetti, *Phys. Med. Biol.* **57**, 99 (2012).

[3] H. Paganetti *et al.*, *Int. J. Radiat. Oncol. Biol. Phys.* **53**, 407 (2002).

[4] A. Schiavi *et al.*, *Phys. Med. Biol.* **62**, 7482 (2017).

[5] M. Garbacz *et al.*, Proton therapy treatment plan verification in CCB Kraków using Fred Monte Carlo TPS tool, in: IFMBE Proceedings, vol. 68, 2019.

[6] S. Agostinelli *et al.*, *Nucl. Instrum. Methods Phys. Res. A* **506**, 250 (2013).

[7] G. Battistoni *et al.*, *AIP Conf. Proc.* **896**, 31 (2007).

[8] A. Carabe-Fernandez, M. Moteabbed, N. Depauw, H. Paganetti, *Phys. Med. Biol.* **57**, 1159 (2012).

[9] J. Bauer *et al.*, *Radiat. Oncol.* **107**, 218 (2013).

[10] J. Krimmer, D. Dauvergne, J.M. Létang, É. Testa, *Nucl. Instrum. Methods Phys. Res. A* **878**, 58 (2018).

[11] P. Moskal, B. Jasińska, E.Ł. Stępień, S.D. Bass, *Nature Rev. Phys.* **1**, 527 (2019).

[12] V. Ferrero *et al.*, *Sci. Rep.* **8**, 4100 (2018).

[13] C. Richter *et al.*, *Radiath. Oncol.* **118**, 232 (2016).

[14] F. Hueso-González *et al.*, *Phys. Med. Biol.* **63**, 185019 (2018).

[15] P. Moskal *et al.*, *Nucl. Instrum. Methods Phys. Res. A* **764**, 317 (2014).

[16] S. Niedźwiecki *et al.*, *Acta Phys. Pol. B* **48**, 1567 (2017).

[17] P. Moskal *et al.*, *Phys. Med. Biol.* **61**, 2025 (2016).

[18] P. Moskal *et al.*, *Phys. Med. Biol.* **64**, 055017 (mar 2019).

[19] P. Kowalski *et al.*, *Phys. Med. Biol.* **63**, (2018).

[20] D. Sarrut *et al.*, *Med. Phys.* **41**, 64301 (2014).

[21] T. Merlin *et al.*, *Phys. Med. Biol.* **63**, (2018).

[22] J. Smyrski *et al.*, *Nucl. Instrum. Methods Phys. Res. A* **851**, 39 (2017).